



ARTICLE



# Integrated geophysical investigation for the characterisation of valley bottom soil at Ilora, Southwestern Nigeria

M. A. Oladunjoye , A. Adefehinti and O. R. Akinrinola

University of Ibadan, Department of Geology, Ibadan, Nigeria

## ABSTRACT

Hydromorphic soils have potential for sustainable agricultural production due to shallow water deposition, accumulation of organic matter and residual available moisture for farming during dry season. Integrated geophysical investigations comprising Ground Penetrating Radar (GPR) and Vertical Electrical Sounding (VES) were conducted on a valley bottom soil at Ilora, Southwestern Nigeria to determine subsurface geometry, lithology and water table in relation to its agricultural significance. Seventeen GPR profiles were established while twenty eight VES were conducted using Schlumberger array. Three test pits were excavated to a depth of 1 m for ground truth. Horizons revealed on the GPR are; sub-parallel reflections assumed to be fine muddy sand rich in organic matter, low amplitude and weak reflections indicating attenuated signal because of high moisture content and multiple chaotic, non-parallel reflectors. The VES results show system of two to four geo-electric layers with average overburden thickness of about 7 m. The excavated pits show intercalation of clayey and loamy soil and revealed water level to be 0.8 m. The integrated geophysical approach applied has successfully identified the spatial pattern of clayey soil, overburden thickness and water level of the valley bottom soil which help retention of water during dry season.

## ARTICLE HISTORY

Received 21 May 2020  
Revised 31 October 2020  
Accepted 29 November 2020

## KEYWORDS

Hydromorphic soils;  
geophysical investigation;  
subsurface geometry;  
internal geometry;  
agricultural significance;  
moisture content

## 1. Introduction

Recently, an increase in agricultural activities led to the use of valley bottom otherwise known as wetlands/hydromorphic soils for agricultural purposes especially during the dry season. The valley bottom is very abundant in Nigeria but they are being under-utilised because of poor understanding of the nature and properties of these soils. It is beneficial to humans' socio-economic activities, environments and also plays significant role in natural ecosystems (Roggeri 1995; Silvius et al. 2000; Stuij et al. 2002). Valley bottom is characterised by water saturation and is regularly flooded during rainy season. Water in the valley bottom is supplied by rain, run-off and base flow from the uplands and fringes, and also drainage from inland valleys further upstream. The hydromorphic fringes, the density and type of vegetation in the upland area, the types of soil found in the watershed, the shape of the inland-valley and the intensity and frequency of rainfall determine the period of flooding (Wopereis et al. 2009). The soil morphological and chemical properties are been affected by persistent water saturation and seasonal alternation between water logging and water draining. The brownish, greyish, bluish, blackish and yellowish mottle colouration often displays by hydromorphic soil during the wet period is as a result of oxidation of iron, manganese and sulphur. Valley bottom is characterised with thick

vegetation and relatively flat lands and heavy soils which make it function as sponges that accumulate water and nutrients during rainy season and maintain subsurface flow during dry season (Dugan 1990; Roggeri 1995). The soils found within valley bottom are very rich in soil nutrients and have high water-holding capacity which makes it good for agricultural purpose (Fagbami and Ajayi 1990). Andriesse (1985) grouped the valley bottom or hydromorphic soils of the basement complex of Sub-Sahara African into narrow headwater inland valleys.

The image of the subsurface stratigraphy can be spatially obtained with diverse geophysical methods like seismic, electrical resistivity, electromagnetics and ground-penetrating radar. Electrical resistivity, electromagnetic and GPR are the common geophysical methods used for river sediment studies because they give significant magnitude of disparity in their physical property contrast than other methods such as seismic velocity and density (Reynolds 1997).

Electrical resistivity and GPR methods present have numerous gains over orthodox soil and sediment investigation methods such as pittings, coring, or trenches. GPR provides high resolution and continuous traverses of the subsurface when properly used in the right environments while resistivity gives detailed information about the earth stratification. This yields a much greater amount of information than discrete sampling by coring or digging (Mokma et al. 1990;

Poole et al. 1997; Conyers and Goodman 1997). Even when excavation is necessary in some manner, GPR and electrical resistivity can aid in the selection of coring sites, maximising effort in areas of interest or uncertainty (Mellet 1995; Augustinus and Nichol 1999). For its non-destructive nature, GPR is valuable in sensitive research settings, such as archaeological sites or protected ecological areas. Also, electrical resistivity method has been found useful in groundwater exploration, mineral exploration, archaeological sites and geo-techniques. In general, GPR and electrical resistivity are efficient tools that give researchers the ability to “see” underground (Harry 2009).

Electrical resistivity method has been widely applied in investigating sub-surface condition by measuring soil or rock electrical properties. Electrolytes or metals conduct electrical resistivity more than insulating material such as air, plastic and deadwood because of their ability to allow the passage of flux of electrical charges. The soil material has intermediate electrical properties but it can be influenced by its physical such as texture, grain size and chemical properties like salinity or water content, (Samouëlian et al. 2005). Electrical resistivity has found various applications in the field of engineering and science. It has been used in delineating the stratigraphy of soil and rock (Ikah et al. 2009), in mapping bedrock and groundwater aquifer (Oladunjoye et al. 2019), in estimating soil and rock permeability (Scott and Emily 2009). Various researchers have used geophysical techniques to delineate diverse sub-surface geometry and conditions. The ground electrical resistivity, electromagnetic, GPR and magnetic methods are very useful in agricultural research (Allred 2011). The variations in dielectric properties of the near surface lithology can easily be identified by GPR with the use of high frequency electromagnetic (EM) wave ranges between 10 and 1000 MHz (Neal 2004). The GPR is often used to map hydro-facies because; at higher frequencies of measurement, the spatial resolution is better, better boundaries detection and rapid measurement time (Topp et al. 1980; Van Dam and Schlager 2000). However, it is generally accepted that low conductive layers can extremely diminish GPR reflections, and thereby reduce the depth of penetration (Bristow and Jol, 2003; Heteren et al. 1998; Theimer et al. 1994). This circumstances offer an advantage to easily identify alluvial fill thickness (Leclerc and Hickin 1997). Consequently, GPR offers pluses as a result of its relative non-sensitive to changes in pore water chemistry, and its provision of high-resolution images that enable a better interpretation of GPR results (Binley et al. 2001). The GPR has been used in investigating soil depth limited by bedrock (Davis and Annan 1992), hard pan thickness, shallow water table and mapping shallow sub-surface soil features such as

estimation of moisture contents in vadose zone, delineating coarse layer in sandy soil zone and evaluating nitrogen loss through the subsurface pathway as it affects agricultural production (Doolittle and Collins 1995; Minet et al. 2011). The electrical resistivity method have been used in mapping internal geometry of river flood plain (Adabanija and Oladunjoye 2014), and used in delineating peat thickness in peat soil of tropical region where traditional coring methods resolution is not feasible (Comas et al. 2015). Also, (Gourry et al. 2003) used integrated geophysical methods of EM profiling, electrical resistivity sounding, electrical resistivity tomography in investigating alluvial bodies and mapping of the presence of clayey-peaty paleochannels.

The present investigation expects to determine geo-electrical parameters and degree of saturation of a typical valley bottom soils using vertical electrical sounding, discriminating between different types of soil horizon by contrasts in their dielectric permittivity and also to relate the geo-electrical parameters and the dielectric contrast between various layers with groundwater level.

## 2. Site description and geological setting

The study was carried out in Ilora near Oyo town, Southwestern Nigeria. It lies between Longitudes 7° 48' 45"N and 7° 48' 55"N and Latitudes 3° 52' 55" E and 3° 53' 05"E (Figure 1) with an estimated area of 81,888.4 m<sup>2</sup>. The southern part of the area was used for fish farming with several fish ponds, with an estimated area of 55,380.1 m<sup>2</sup> covering two-third of the total area, while the north-western part is a vegetable farm with an estimated area of 26,507.5 m<sup>2</sup>. The study area is surrounded by poultry farms. Accessibility of the study area is through a lateritic road that links Ilora and Obanako.

(NIMET 2008) observed from the rainfall and temperature data collected from 1941 to 2000 that there has been shift from “early to normal” the commencement and early cessation of rainy (wet) season in Nigeria. The report established the decline in the period of rainy season in Nigeria while the annual total rainfall is practically unchanged, thereby resulting in floods and drought incidences. The study location falls within the tropics and thus characterise with rainy (wet) and dry seasons. The annual rainfall of about 1420.06 mm is being experienced in the area while 26.46°C was reported as the mean annual temperature with 74.55% as the relative humidity (NIMET, 2011). The rainy season is experienced from March – mid July and late August to late October. Between mid-July to early August there exist short dry season while prolonged dry season is experienced from November to March (Akinseye, 2010). The late commencement and early cessation of rainy season around the study

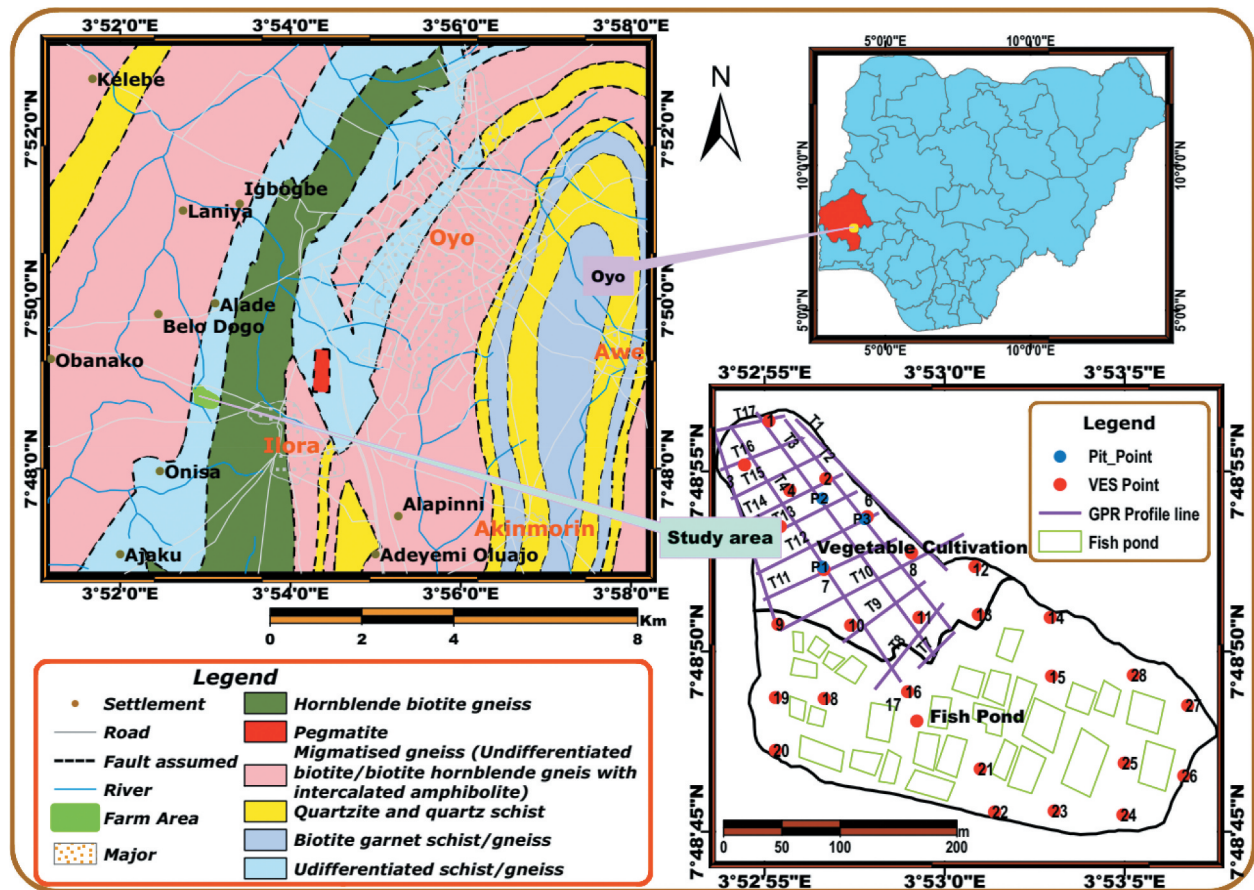


Figure 1. Geological and location maps of the study area and its environs (Source: NGSA, 2009).

location makes the valley bottom to be of high agricultural value.

The study area topography is generally rough and near flat with no visible rock exposures. The drainage pattern is typically dendritic, characterised by irregular branching of the tributaries and flow direction is typically towards the north. Most of the streams have dried up during the research work with mud cracks indicating evaporation of water from clay materials derived from the weathered rocks around the study area.

### 2.1. Geology of the study area

The rock type underlying the study area is gneiss which occurs massively with medium to coarse grain texture. The rock is marked with alternating melanocratic and leucocratic minerals aligned in defined foliation plane. Most of the outcrops observed were migmatite gneiss (Figure 1) and granite gneiss having quartz veins of varying widths. Pegmatite is common as intrusive rock which occurs as dyke or vein filling the joints and sheared zones. They weathered easily to clay and sand size particles, which has low permeability and serve as water retention zone (Palacky et al. 1981). The area investigated is underlain by banded gneiss which was part of the area classified as undifferentiated gneiss

complex (Jones and Hockey 1964). The banded gneiss around this area is marked by alternating hornblende-biotite rich bands and quartz-oligoclase rich bands (Burke et al. 1976). The banded gneiss which derived its origin from sedimentary sequences, contain large lenses of granite gneiss and thin-intercalated layers of quartzite and amphibolite (Burke et al. 1976).

### 3. Materials and methods

Reconnaissance survey was done to determine the area extent of the valley bottom with the aid of GPS and also to map its accessibility for the deployment of geophysical equipment for data acquisition. The reconnaissance survey also helped to ascertain the state of saturation of the study area so as to plan for the operation of geophysical equipment. The vertical electrical sounding points and the GPR profiles were spatially distributed as space permits (Figure 1). The GPR was only carried out in areas where fish ponds were not cited for easy accessibility of equipment while the vertical electrical sounding was done across the study area. Three trial pits were established on selected GPR profiles to ground truth the geophysical results.



### 3.1. Electrical resistivity method

Generally, electrical resistivity method is being deployed with two pairs of electrode, the current which is the outer electrode and the potential which is inner electrodes. Electric current was injected to the subsurface via the outer electrodes and potential difference was passed across the inner electrodes and the resultant electrical resistance was then recorded from the resistivity metre. The depth of penetration of the electric current in homogeneous subsurface is directly proportional to the spacing that exist between the pair of current electrodes. The subsurface information of the point being investigated is revealed by varying the spacing between the pair of current electrodes, (Koefoed 1979). The VES data were acquired by means of Schlumberger electrode array. Twenty eight VES data were spatially acquired across the study area with half electrode spacing of 100 m. Campus Tigre resistivity metre was used in acquiring the resistivity data with observed error being less than 1 %.

The interpretation was done by manually plotting the acquired data on bi-log graph so as to permit large variation in resistivity value and half electrode spacing on the same graph. The techniques of Zohdy (1965) and Orellana and Mooney (1969) were applied to curve match the plotted data while IPIWin software was used in the final stage of interpretation. The derived model from the software was used to generate geo-electric parameters which are topsoil resistivity, overburden thickness, weathered layer resistivity, basement topography, and basement resistivity.

### 3.2. Ground-penetrating radar

The GPR reflection data were acquired with the aid of SIR system-3000. Antenna frequency of 400 MHz which is expected to give good resolution of the geometry and the target depth was used. Seventeen profile lines were established for this study, six were acquired in northwest – southeast direction with 50 m inter profile spacing while eleven were acquired in northeast – southwest direction with 20 m inter profile spacing (Figure 1). For data acquisition, sixty four scans per seconds and 25 scan per metre with a sampling window of 120 nano seconds (ns), and range of 100 ns and 5 point gain was used. Calibration for the GPR data positioning was done with the survey wheel and each radar trace contained 1024 per trace with 16 bits/sample. A dielectric constant of 16 with Vertical Low Pass Filter of 800 MHz and Vertical High Pass Filter 100 MHz was used due to nature of the study area.

To remove unwanted very low-frequency noise the data was dewowed by applying temporal filtering.

Time zero shift was applied to correct for time drift which helped to accurately position the GPR reflections on the vertical scale (Lejzerowicz et al., 2014). A band-pass filter was applied to subdue noises with frequencies differ from that of the signal. It helps to get rid of unwanted noise at low and high ends of amplitude spectrum (Best et al., 2006; Cassidy and Jol, 2009). The GPR data were deconvolved to the best of the bandwidth and decrease the pulse dispersion so as to get the best resolution. Static correction was done on the data so as to time – shift the record for first signal arrivals. Automatic gain was applied so as to compensate for the signal attenuated with depth.

Different horizons were delineated with lines of different colours on each radar section. This was done based on the continuity of reflections and accompanied by colouring each layer. (Busby et al. 2004) surmised that GPR data interpretation is generally empirical and it depends on the ability of the interpreter to identify reflections' configurations and patterns on the radar section. Basically, GPR data interpretation depends on the pattern of reflections and the strength or the sharpness of the reflection signals. GPR data interpretation was centred on the continuity of horizontal events, hyperbolic reflections and chaotic reflections. The interpretation of the GPR results obtained from the processed data were achieved by considering the succession of the stratigraphy observed on the radar facies centred on the amplitude and continuity of the reflections and basic knowledge of the local geology in correlation with hand dug pit log obtained in the area.

### 3.3. Ground truthing

Direct human observation is a particularly effective ground truthing method and is most often used in the field of geophysics to validate geophysical interpretation. It helps to identify areas of discrepancy and provide bases for model revisions where necessary. Depending on the complexity of the investigation and the degree of accuracy required, two or more ground truth may be employed to refine the geophysical model.

For this study, the ground truthing was done by direct observation on the nature of material that underline the study area through excavation. Three pits (Figure 1) were established on selected GPR profiles and VES points. Pit 1, 2 and 3 were established on VES7 along with GPR Profile 4, along GPR profile 3 and on VES 6 at the intersection of GPR profiles 2 and 12, respectively. During pitting, rapid assessment was made on the excavated samples collected from the pit by visually observing each horizon of the pit. The maximum depth recorded for the pits was 100 cm which was equivalent to static water level in the study area.



## 4. Results and discussion

### 4.1. Geo-electrical investigation

The VES curves were generated from the processed electrical resistivity field data. Two to four geo-electrical layers were obtained from the electrical soundings as summarised in Table 1. The results of the electrical sounding presented two to four geo-electrical layers as summarised in Table 1. Topsoil resistivity map, overburden thickness map, weathered formation resistivity map, basement resistivity map, and basement relief/topography map were generated from the interpreted VES data. Similarly, the interpreted result was also used to correlate with the GPR result and the log from the pitting.

#### 4.1.1. Topsoil resistivity

The variation in the topsoil resistivity is shown in Figure 2 and gives an insight into the materials that constitute the topsoil within the study area. The topsoil resistivity ranges from 4  $\Omega\text{m}$  to 1037  $\Omega\text{m}$  (Table 1) with mean value of 177  $\Omega\text{m}$ . The large variation in the topsoil resistivity was due to different soil compositions that form the topsoil. The topsoil resistivity at the northwestern part of the study area was less than 100  $\Omega\text{m}$  which was interpreted as saturated clayey materials (Reynolds 1997) while the topsoil at the southeastern part of the area was dominated by materials of resistivity greater than 400  $\Omega\text{m}$  which was interpreted as lateritic clay (Telford et al. 1990; Reynolds 1987a, McGinnis and Jensen 1971). The topsoil at the central part is dominated by low

resistivity materials of between 100 and 200  $\Omega\text{m}$  which was interpreted as sandy clay/clayey sand material (Telford et al. 1990; Reynolds and Paren 1980, 1984) which was visible at the surface during field exercise. The clay dominated topsoil in the northwestern part of the area was also observed during pitting.

#### 4.1.2. Overburden thickness

The average overburden thickness was 7 m which means that it was generally shallow around the area. The thickness of the overburden at the northwestern part was greater than 15 m while at the south and southeastern parts, the overburden was shallow at less 10 m. The thickness of the overburden at the northeastern area fell within the range given by Omosuyi et al. (2003), Dan-Hassan and Olorunfemi (1999) and Olorunfemi and Okhue (1991) and can store groundwater while the south and the southeastern parts fell short of the range. The soil materials of the overburden at the northeast (Figure 3) have high water retention capacity which serves as source of water for the valley bottom during dry season.

#### 4.1.3. Weathered layer formation resistivity

The variation in weathered formation resistivity of the area is shown in Figure 4. This resistivity ranges from 4  $\Omega\text{m}$  to 80  $\Omega\text{m}$  with average resistivity of 21  $\Omega\text{m}$ . The least resistivity value of weathered formation was observed at the centre and the northwestern part while high resistivity value of weathered formation resistivity was observed at the southern part. Based on Adiat et al. (2009), the whole study area can be considered to have

**Table 1.** Summarised geo-electrical parameter derived from the VES curves from the study area.

| VES No | Resistivity ( $\rho$ ) ( $\Omega\text{m}$ ) | Thickness (h) (m) | Reflection coefficient | Lithology  |
|--------|---|-------------------|------------------------|--|
| 1      | 27/10/375                                   | 1/3.1             | 0.95                   | Topsoil/Saturated clay/Fresh basement                    |
| 2      | 34/12/605                                   | 1.1/5.8           | 0.96                   | Topsoil/Saturated clay/Fresh basement                    |
| 3      | 15/395                                      | 1.2               | 0.93                   | Topsoil(Saturated clay)/Fresh basement                   |
| 4      | 4/744                                       | 2.3               | 0.99                   | Topsoil(Saturated clay)/Fresh basement                   |
| 5      | 6/439                                       | 1                 | 0.97                   | Topsoil/Fresh basement)                                  |
| 6      | 8/57/840                                    | 1.6/4.4           | 0.88                   | Topsoil/Saturated clay/Fresh basement                    |
| 7      | 10/208                                      | 1.5               | 0.91                   | Topsoil(Saturated clay)/Fresh basement                   |
| 8      | 244/15/364                                  | 1/7.5             | 0.92                   | Topsoil/Saturated clay/Fresh basement                    |
| 9      | 9/272                                       | 1                 | 0.94                   | Topsoil/Fresh basement                                   |
| 10     | 6/636                                       | 2.8               | 0.98                   | Topsoil/Fresh basement                                   |
| 11     | 22/11/330                                   | 1.1/3.5           | 0.94                   | Topsoil/Saturated clay/Fresh basement                    |
| 12     | 102/566/11/246                              | 0.6/1.4/6.7       | 0.91                   | Topsoil/Lateritic clay/Saturated clay/Fresh basement     |
| 13     | 121/18/163                                  | 0.4/8.2           | 0.8                    | Topsoil/Saturated clay/Fresh basement                    |
| 14     | 367/2744/80/482                             | 0.6/2.2/6.3       | 0.72                   | Topsoil/Lateritic clay/Saturated clay/Fractured basement |
| 15     | 93/276/12/251                               | 0.8/1.3/6.3       | 0.91                   | Topsoil/Lateritic clay/Saturated clay/Fresh basement     |
| 16     | 43/06/298                                   | 1/4.8             | 0.96                   | Topsoil/Saturated clay/Fresh basement                    |
| 17     | 77/18/234                                   | 1.4/6.5           | 0.86                   | Topsoil/Saturated clay/Fresh basement                    |
| 18     | 135/14/378                                  | 1/6.1             | 0.93                   | Topsoil/Saturated clay/Fresh basement                    |
| 19     | 11/244                                      | 1                 | 0.91                   | Topsoil(Saturated clay)/Fresh basement                   |
| 20     | 127/18/293                                  | 0.8/4.7           | 0.88                   | Topsoil/Saturated clay/Fresh basement                    |
| 21     | 9/65/6/544                                  | 0.5/1.3/4.6       | 0.98                   | Topsoil/Clay formation/Saturated clay/Fresh basement     |
| 22     | 270/1353/41/245                             | 0.6/1.8/11.7      | 0.71                   | Topsoil/Lateritic clay/Saturated clay/Fractured basement |
| 23     | 723/542/45/280                              | 1.2/2.2/15.7      | 0.72                   | Topsoil/Lateritic clay/Saturated clay/Fractured basement |
| 24     | 706/28/305                                  | 1.2/7.8           | 0.83                   | Topsoil/Saturated clay/Fresh basement                    |
| 25     | 48/21/354                                   | 1.5/7.7           | 0.89                   | Topsoil/Saturated clay/Fresh basement                    |
| 26     | 44/165/24/396                               | 1/2.4/6.8         | 0.89                   | Topsoil/Lateritic clay/Saturated clay/Fresh basement     |
| 27     | 683/34/321                                  | 1/9.3             | 0.8                    | Topsoil/Saturated clay/Fresh basement                    |
| 28     | 1037/43/444                                 | 1.4/10.1          | 0.82                   | Topsoil/Saturated clay/Fresh basement                    |

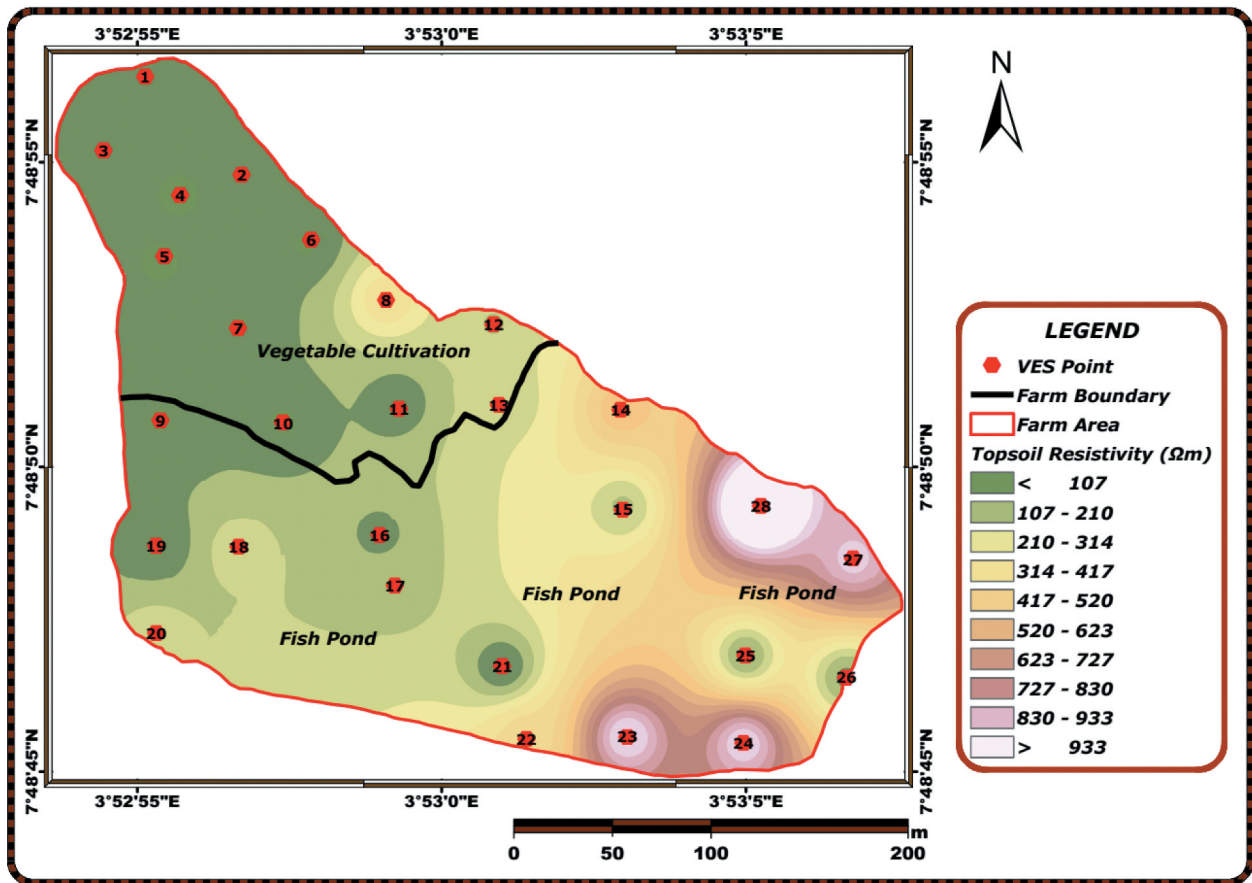


Figure 2. Variation in topsoil resistivity of the study area.

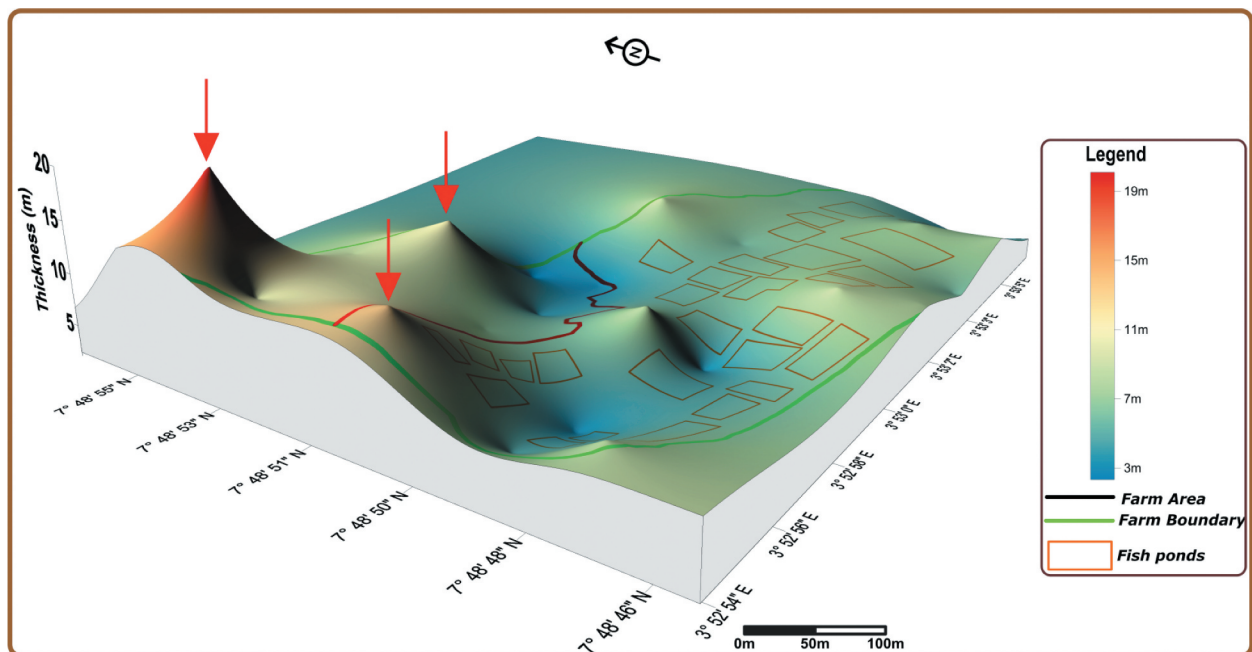


Figure 3. Variation in overburden thickness map across the study area with the arrows showing area with thick overburden.

poor groundwater prospect except some southeastern part due to the resistivity value of the dominant soil materials (Figure 4). The material which is clayey in content has poor permeability and thereby do not release water easily after absorbing it which makes it good for the dry season farming in the floodplain area.

#### 4.1.4. Basement/Bedrock resistivity

Bedrock resistivity map (Figure 5) is being overlaid with reflection coefficient contour line. The resistivity values of the basement in the study area vary between 163 and 840  $\Omega\text{m}$  with average resistivity of 381  $\Omega\text{m}$  while the reflection coefficient values vary between

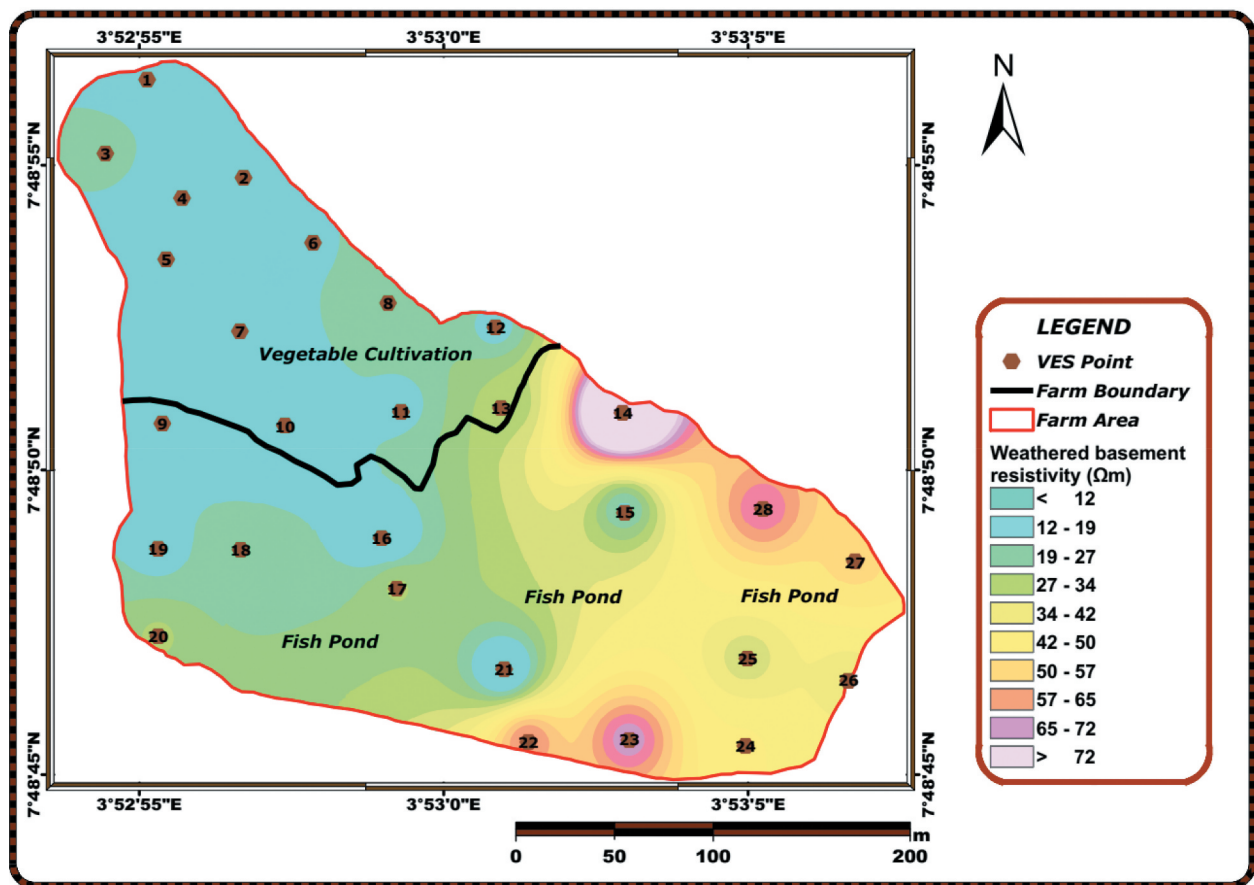


Figure 4. Variation in weathered layer formation resistivity of the study area.

0.71 and 0.99 with average of 0.89. The freshness of the basement in this study was determined by overlying and correlating the basement resistivity map and reflection coefficient (Table 1) contour line of each VES. The reflection coefficient was estimated using the formula proposed by Bhattacharya and Patra (1968) and Olayinka (1996). The basement is considered to be fresh if it has resistivity value greater than 1000  $\Omega\text{m}$  and reflection coefficient value greater or equal to 0.8 (Olayinka 1996). As observed in Figure 8, the Southeastern part was dominated by fractured basement because it was characterised with basement resistivity of less than 500  $\Omega\text{m}$  and the reflection coefficient less than 0.8. The northwestern part of the study area was characterised with basement resistivity less than or equal to 500  $\Omega\text{m}$  and the reflection coefficient greater than 0.8 and the basement here is termed partially fractured basement. The central part of the area was dominated by fresh basement because it has basement resistivity less than 1000  $\Omega\text{m}$  with high reflection coefficient greater than 0.9.

#### 4.1.5. Basement/Bedrock relief (Topography)

Figure 6 shows variation in basement relief map obtained from the VES results. This map displayed the present basement topography which is an indication of degree of chemical weathering within the bedrock. Basement depressions and ridges were

identified in the relief map. The depression was considered to be overlain by thick overburden and correlated with fractured/partially fractured basement (Figure 6) as seen in the northwest. The ridges were overlain by thin overburden as observed at the south-east while the central part of the map is of moderate height and slopes towards the northwest. As observed from the basement resistivity map (Figure 6), the central part which has moderate height is underlain with fresh basement from the basement resistivity and reflection coefficient values. In addition, being overlain by thick overburden, basement depressions also constitute groundwater accumulating troughs, for water displaced from the bedrock crest. The northwestern part around VES 1, 2, 3, 4, 5, 6, 7 and 8 will be good groundwater accumulating centre as they are located within the depression of the basement topography. Naturally, groundwater flows from bedrock ridges where there is high pressure to bedrock depression where the pressure is low. Consequently, bedrock depressions will play significant role in groundwater development. The northwestern part of the study area which has basement depression serves as water-collecting centre where clay materials that constitute the weathered basement can absorb water from and store for a very long time which can then support farming during long period of dry season.



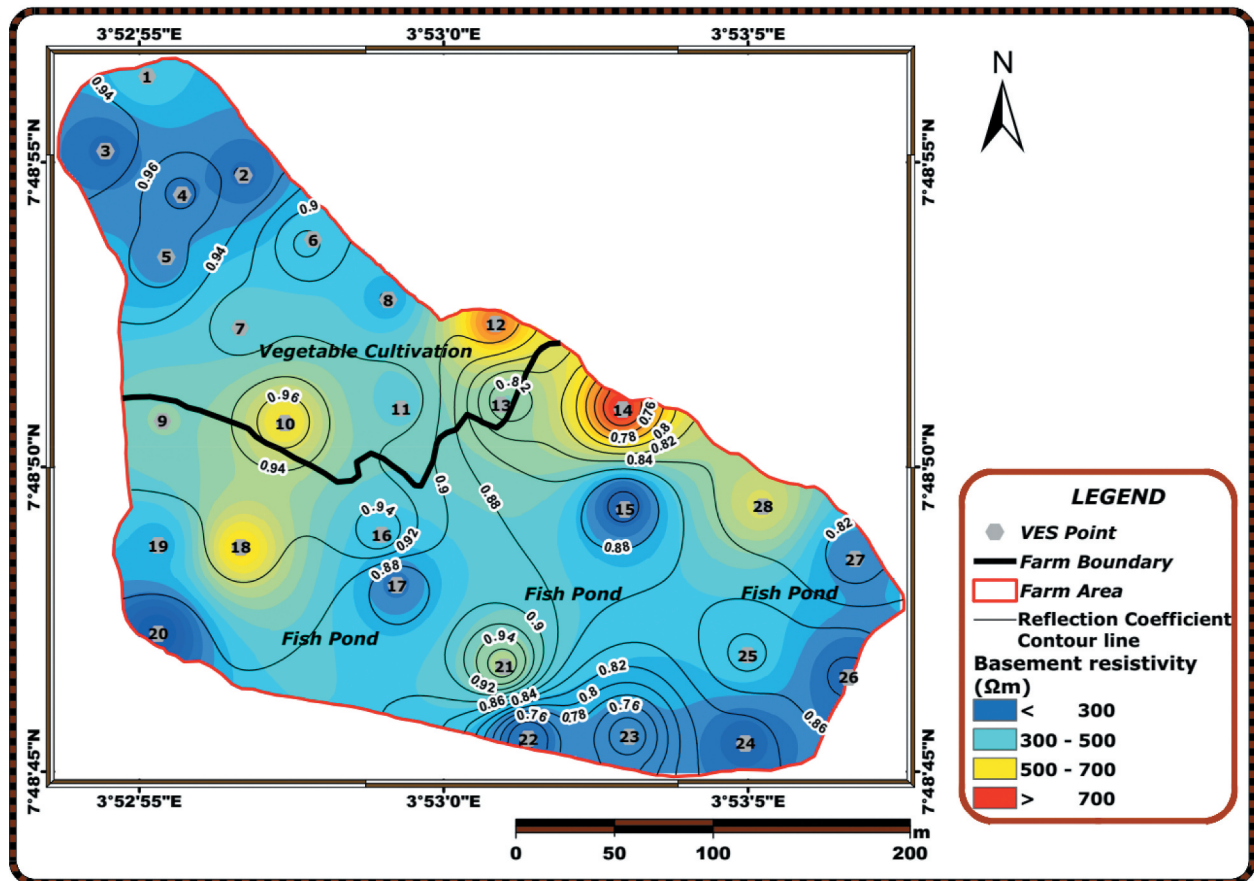


Figure 5. Variation in basement/bedrock resistivity and reflection coefficient contour.

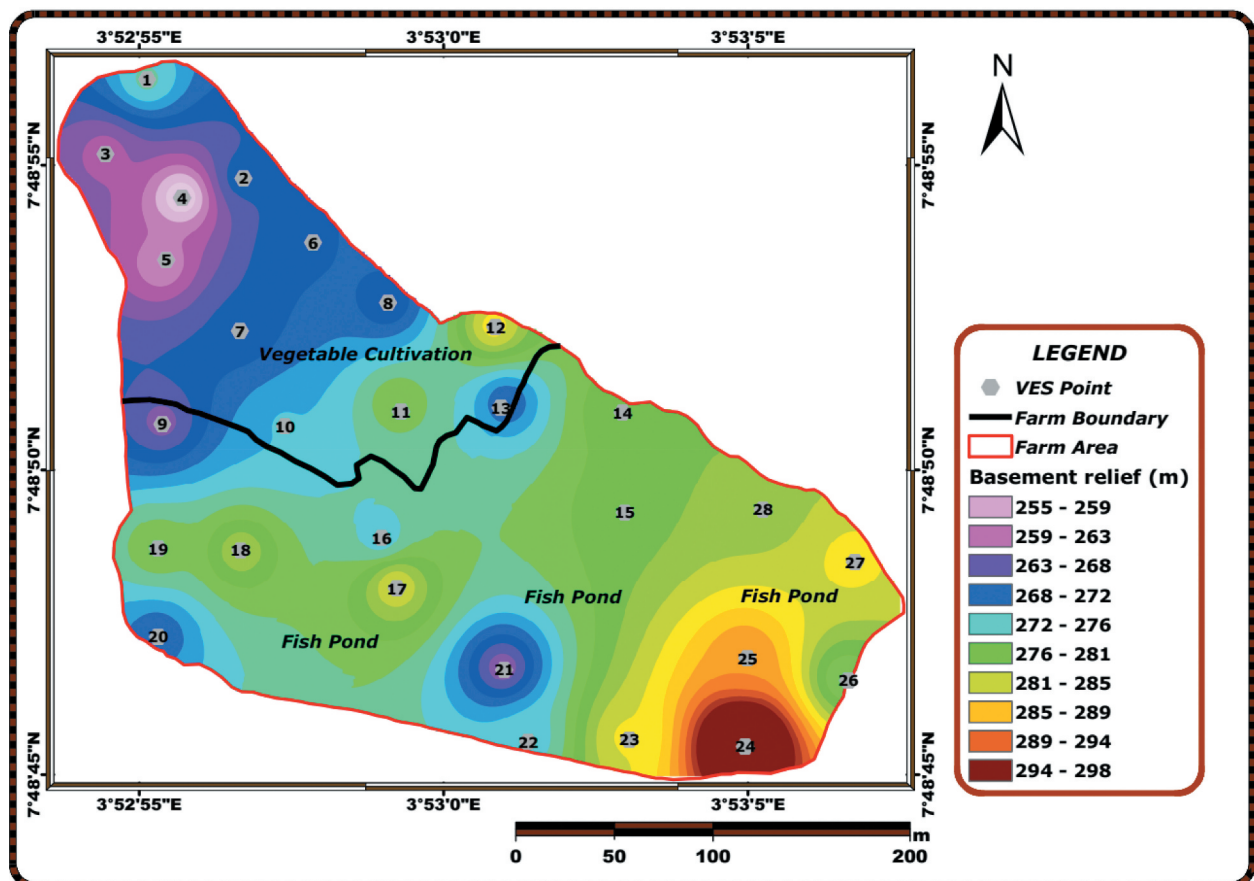


Figure 6. Variation in basement relief of the study area.

## 4.2. Ground-penetrating radar investigation

Generally, to characterised ground conditions in any geological environment, the most effective geophysical method is GPR (Hong et al. 2018). Figure 7–10 show representatives of processed radar sections for profiles acquired in northwest – southeast direction and northeast – southwest direction, where three reflecting surfaces were identified and picked manually. The anomalies observed on the GPR images obtained at both directions showed each layer mapped has dissimilar electromagnetic properties of the ground. The principles of radar stratigraphy proposed by Beres and Haeni (1991) which were copied from seismic stratigraphy (Mitchum et al. 1977) were used to characterise the radar sections. Three litho units labelled horizons 1 to 3 were identified from all the sections based on distinct GPR signal reflections. The horizons are the mappable 2-d units, that have common characteristics such as internal reflection pattern, shape, amplitude, continuity and external 2-D form that differs from neighbouring units using the methodology suggested by Beres and Haeni (1991), Heteren et al. (1998); Ekes and Hickin (2001).

The first interface was the topmost layer labelled horizon one, with thickness of about 0.5 m and was characterised by sub-parallel, undular, and variable dip reflections that indicate fine muddy sand which is rich in organic matter, plant remains and clay. This was interpreted to result from channel fill element and flooding of the land surface overtime. Horizon with these attributes is known to have low permeability as a result of the material component that made it (Dara et al., 2019).

The second interface which is of interest because it was observed to be distinct and prominent in the whole radar section and was characterised by low amplitude, continuous and weak/structureless reflections, indicating attenuated signal. The horizon was considered to have high moisture was interpreted as saturated weathered basement which has clayey material as its constituents. The horizon may correspond to

the swamp deposit and such horizon is subject to have low permeability Dara et al., 2019. The saturation of the study area all year round is caused by this layer because of its low permeability which enables it to hold water that are being used for farming during dry season. This layer has thickness range of 0.9–1.4 m. Also observed to be scattered in this horizon are hyperbolic reflections, which sometimes result from point objects within the subsurface. (Dara et al., 2019) observed that such hyperbolic reflections are normally produced by discrete, spatially restricted, non-planar features (point targets) such as rock boulders, sands with organic fragments etc.

The third interface was the weathered basement labelled horizon 3 characterised by multiple chaotic, discontinuous and non-parallel reflectors. Also characterising this region are dipping and basin-like features and non-uniform layer probably due to the variation in topography of the weathered basement. This was interpreted as weathered basement layer characterised with pebbles and cobbles from weathered rock.

The signal strength and resolution around horizon 1 and 3 appear stronger than horizon 2 because of the difference in permittivity and conductivity of the material compositions. Horizons 1 and 3 are dry and so allow for the easy passage of EM wave, horizon 2 on the other hand is saturated and so tends to attenuate EM wave hence the weak and low amplitude reflection signal around this zone. The horizon 2 is characterised with wet clayey materials which is responsible for the attenuation of the EM wave and due to its low permeability, it can retain water for longer period. It supplies the water needed by the plant during dry season and the plants derived their nutrient from this and the topmost zones.

## 4.3. Pitting (ground truth)

Generally, the materials from the three pits range from loam to clayey soil but with different colour. Pit 1 (Figure 11a) has four horizons which has top dry

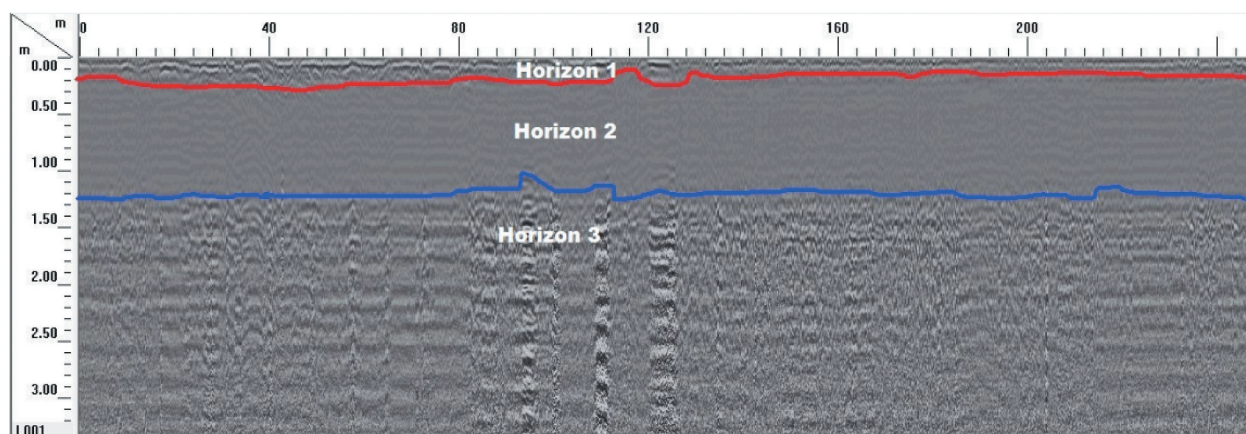
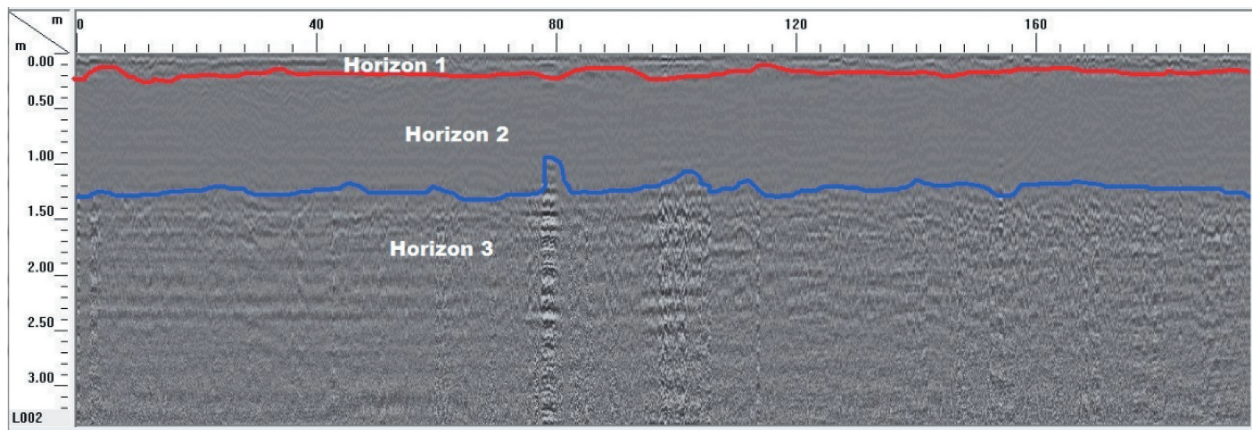
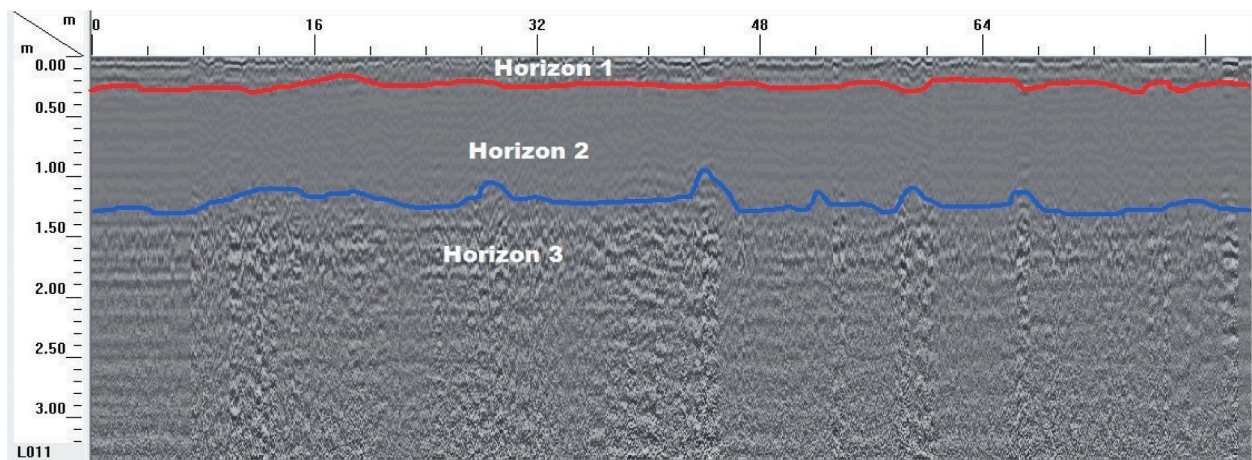


Figure 7. Radar image for profile one along northwest – southeast direction.





**Figure 8.** Radar image for profile two along northwest – southeast direction.



**Figure 9.** Radar image for profile fourteen along northeast – southwest direction.

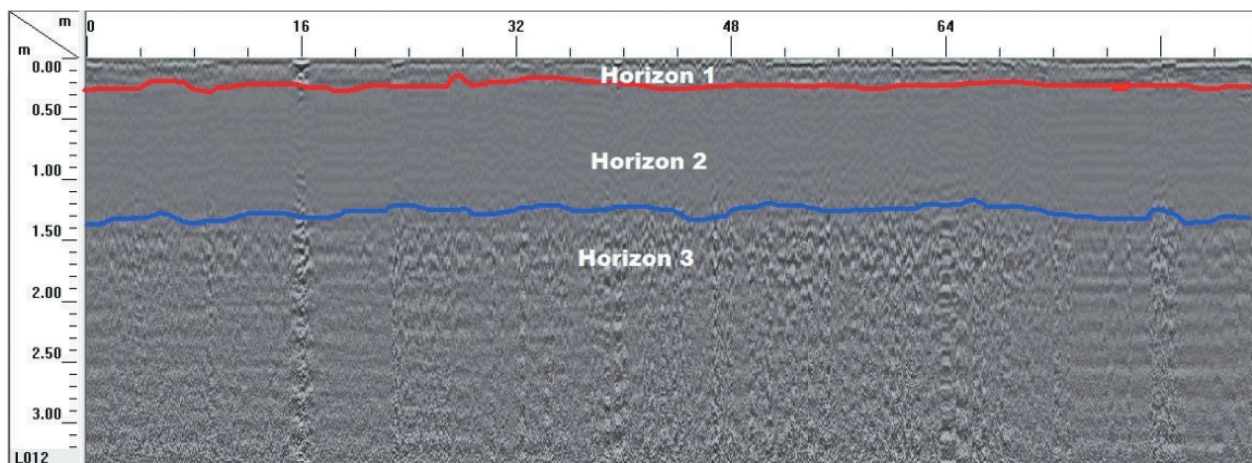


**Figure 10.** Radar image for profile fifteen along northeast – southwest direction.

reddish brown loamy soil, followed by moist brown loamy soil, then dark moist clayey loamy soil and lastly, dark grey wet clayey soil. The water table here was encountered at about 0.8 m. Pit 2 (Figure 11b) has three horizons with top dark grey loamy soil, followed by moist brown loamy soil and lastly, dark grey wet clayey soil. The water table was encountered at about 0.8 m. Pit 3 (Figure 11c) has four horizons which has

brown loamy soil at the top horizon, followed by dark moist loamy soil, then greyish silty soil and lastly, dark grey silty sand. The water table at this pit was encountered at about 0.75 m. The material recovered from the pitting were part of the topsoil and the saturated clay observed from the VES result. The result revealed that the lower part of the topsoil and the layer underlying it is saturated. The water table found close to the surface



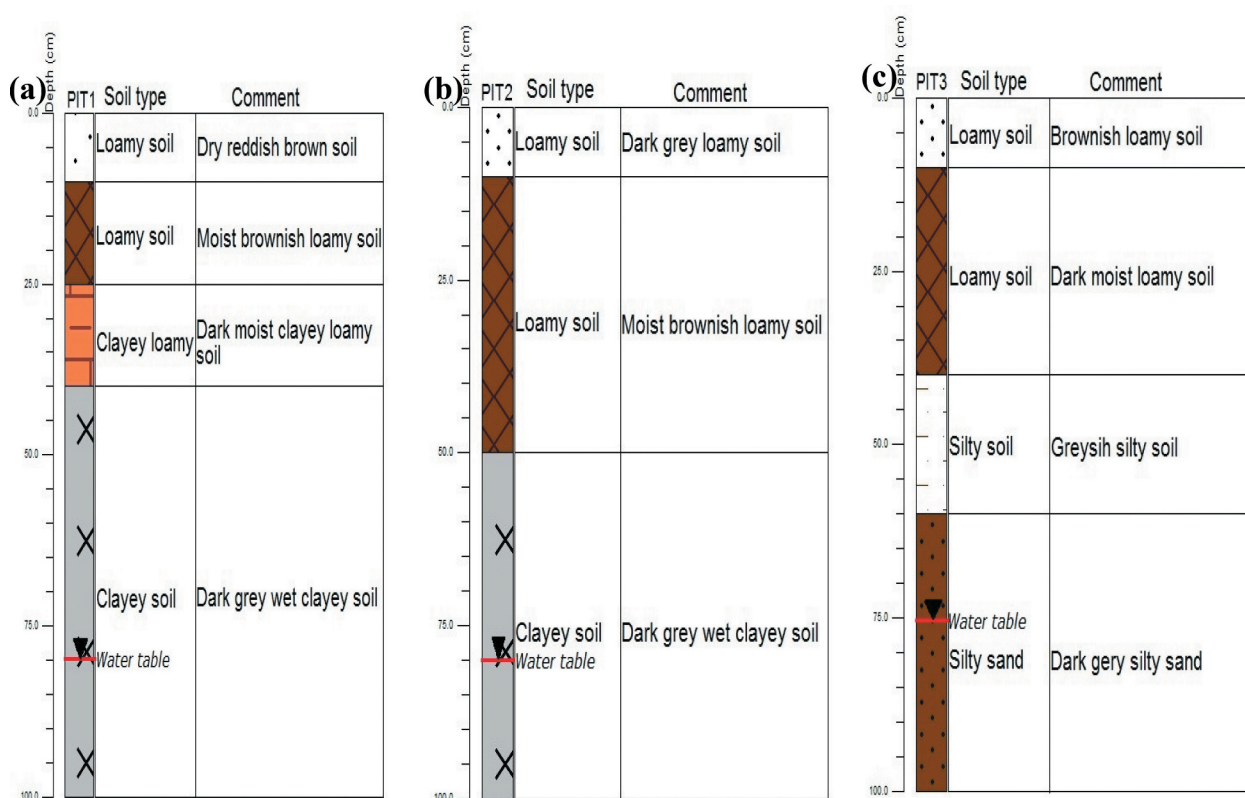


Figure 11. Lithology as revealed in (a) Pit 1, (b) Pit 2, (c) Pit 3 of the study area.

from the ground-truthing corroborates the assumption from the interpretation of the VES result that the topsoil and the layer below it are saturated.

#### 4.4. Correlating VES, GPR and pitting results

The VES result obtained from the northeastern part of the study area where GPR was carried out show that the topsoil is characterised with material of very low resistivity which is less than 100  $\Omega\text{m}$  and such material was interpreted as saturated clay material (Reynolds 1997). This result correlates with observation of low amplitude, continuous and weak/structureless reflections, indicating attenuated signal because the horizon was considered to have high moisture content caused by the

saturation of water in the clayey material from the GPR result. The topsoil observed in VES result correlates with the first two layers identified on the GPR result and was confirmed by the ground truthing result. The ground truthing revealed that the water level is close to the surface which corroborates the observation on the result of GPR and also agree with the inference drawn from the resistivity value for the topsoil and weathered layer formation in the area. It was observed from the ground truthing that most of the base of the GPR sections was occupied by weathered basement which were characterised with pebbles and cobbles.

Figure 12–14 show correlation between the pitting result and the GPR profiles. The pit was found to extend from the first horizon on the GPR profile

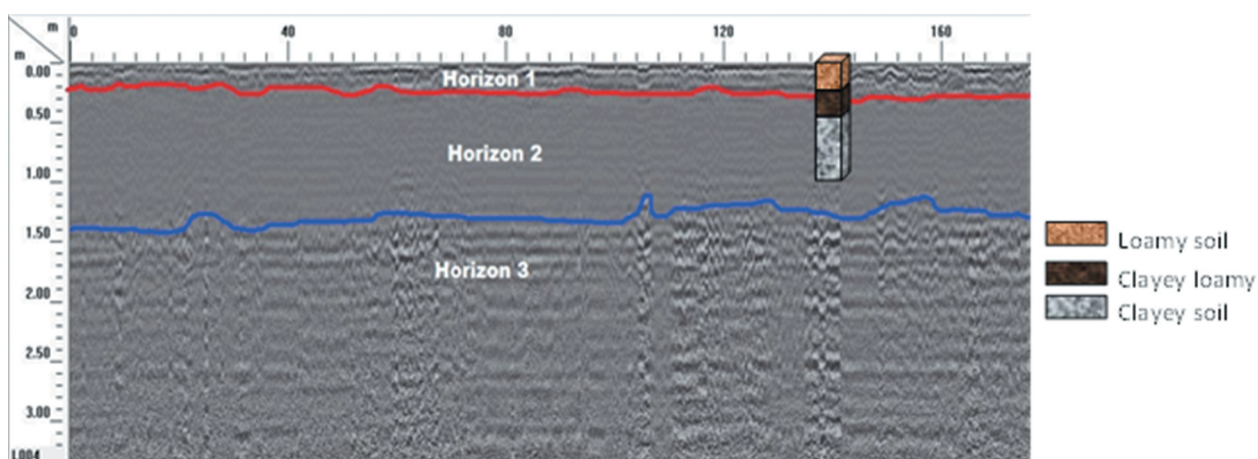


Figure 12. Radar image of profile four along northwest – southeast direction with the logging from pit 1.

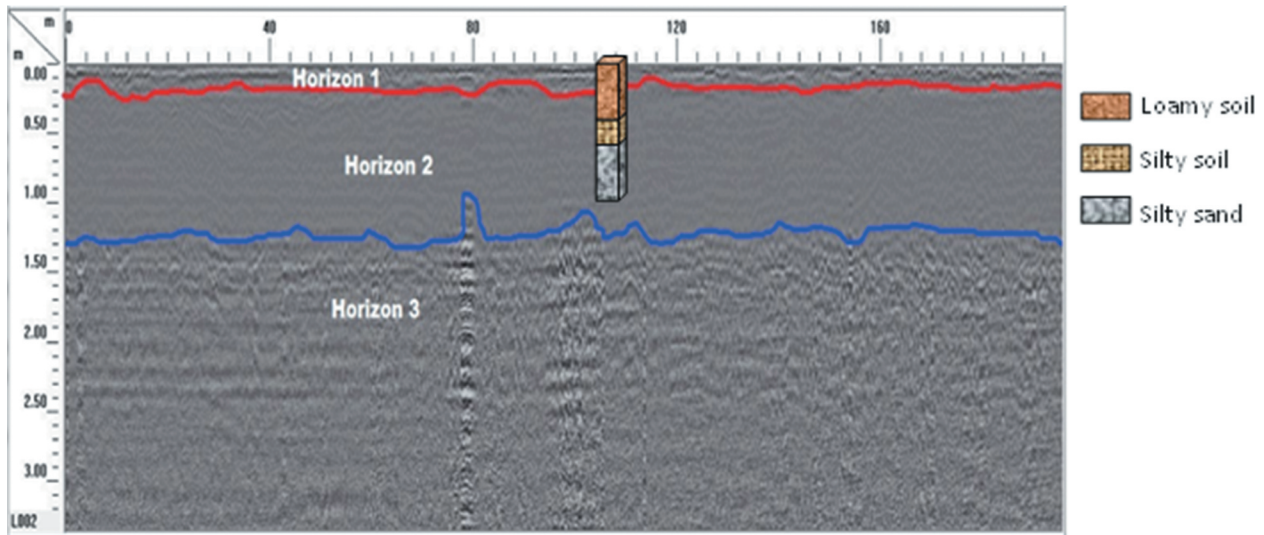


Figure 13. Radar image of profile two along northwest – southeast direction with the logging from pit 3.

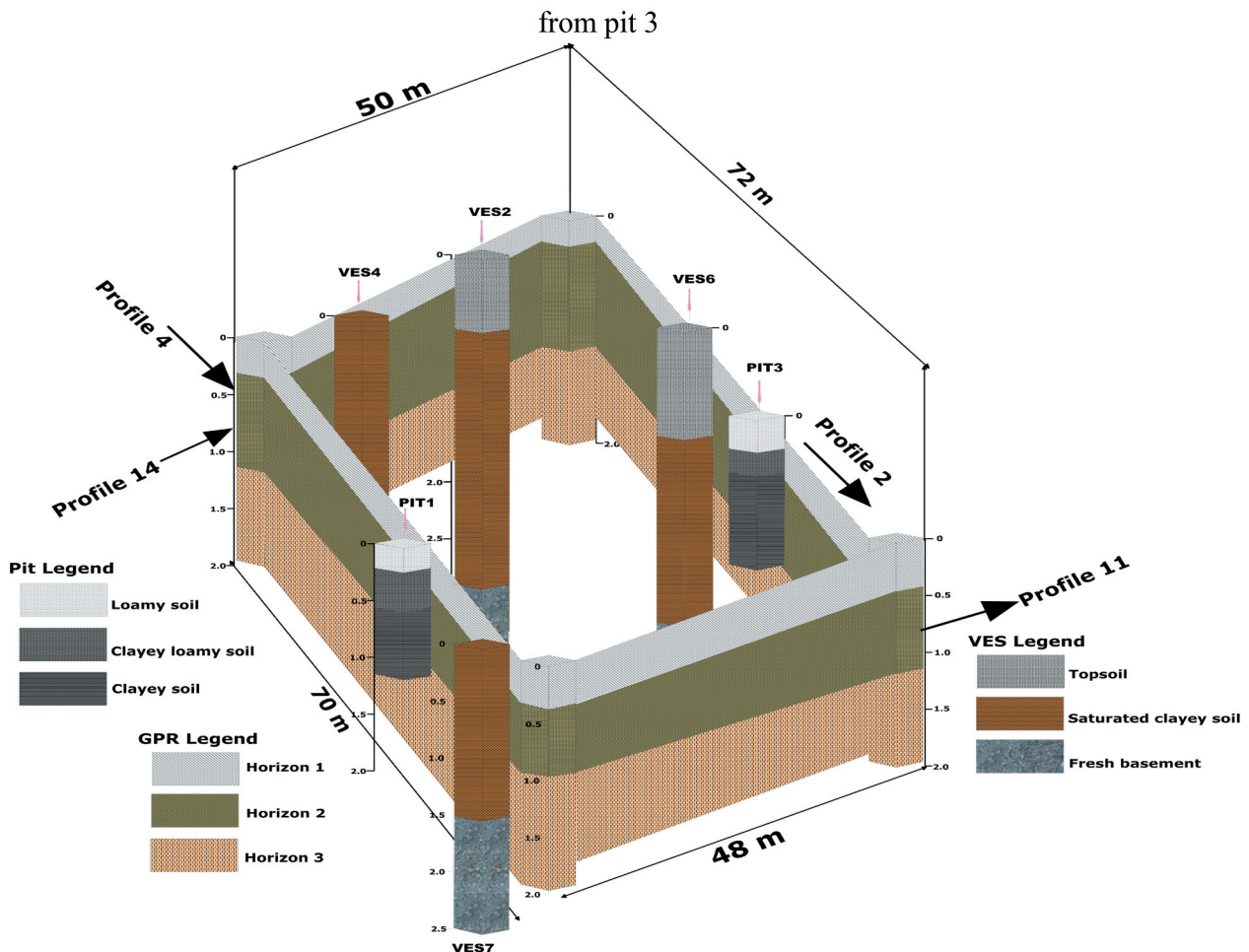


Figure 14. Fence diagram showing the correlation and relationship between GPR profiles, VES points and pits for the study area.

to the second horizon. The first horizon on the GPR profile correlates with the material that forms the top layer of the pit while the second horizon on the GPR profile which was saturated correlates with the latter part of the pit where the material is clayey for pits 1 and 2 and silty for pit 3 which are saturated.

## 5. Conclusions

The valley bottom soils in Ilora, southwestern Nigeria was characterised using electrical resistivity method of Vertical Electrical Soundings (VES) and Ground-Penetrating Radar (GPR) to determine the soil electrical properties and the permittivity of the material component of the soil, respectively. The results from





both methods show three prominent layers in the study area. The layers are; the relatively dry topsoil composed of fine-grained soil (clay, silt) as visibly shown on the radar section and with relatively low resistivity. This was confirmed by the three test pits that established the presence of clayey – silty soil of varying colours from dark to brownish. Below this layer is the water-saturated soil which was revealed on the radar section as low amplitude region caused by signal attenuation as a result of conductive environment. This showed a relatively lower resistivity value in the resistivity result. This zone is important as it held most of the groundwater and due to low permeability of clay soil and most of the water is retained. The basement underlies the saturated clay layer with varying degree of weathering. The freshness of the basement does not allow the percolation of water but enhances weathering or in-situ decomposition of basement which is shown in the radar image and resistivity result. The southern part of the study area has higher basement relief which allows the flow of water to the northwestern part and this allows for weathering of basement which made the overburden in this area to be relatively thick. The integrated geophysical methods was able to successfully reveal the internal geometry, overburden thickness, water level, the condition of basement (fresh or fracture). All these gave the knowledge of the characteristics of the valley bottom soils that makes it to retain water during dry season for agricultural purposes.

## Disclosure statement

No potential conflict of interest was reported by the authors.

## ORCID

M. A. Oladunjoye  <http://orcid.org/0000-0002-6162-4170>  
A. Adefehinti  <http://orcid.org/0000-0002-3121-5026>

## References

- Adabanija MA, Oladunjoye MA. 2014. Investigating Internal geometry of a flood plain in basement complex terrain using electrical resistance tomography. *Int J of Multidisciplinary and Curr Research*. 2:925–926.
- Adiat KN, Olayanju GM, Omosuyi GO, Ako BD. 2009. Electromagnetic profiling and electrical resistivity soundings in groundwater investigation of a typical basement complex- a case study of oda town southwestern nigeria. *J of Applied Sci*. 2(4):333–359.
- Akinseye FM, 2010: Climate variability and effects of weather elements on cocoa and cashew crops in Nigeria, M.Tech Thesis, Unpublished.
- Allred BJ. 2011. Agricultural geophysics: past/present accomplishments and future advancements. *The Second Global Workshop on Proximal Soil Sensing*. 1:24–32.
- Andriesse W, 1985. Wetlands in Subsaharan Africa. Area and Distribution. *International Conference on Wetland Utilization for Rice Production in Subsaharan, Africa*, (15–30). Ibadan.
- Augustinus PC, Nichol S. 1999. Ground penetrating radar imaging of pleistocene sediments, boco plain, western tasmania. *Aus J of Earth Sci*. 46(issue 2):275–282. doi:10.1046/j.1440-0952.1999.00697.x.
- Beres M, Haeni F. 1991. Application of ground-penetrating-radar methods in Hydrogeologie Studies. *Ground Water*. 29:375–386. doi:10.1111/j.1745-6584.1991.tb00528.x.
- Best J, Woodward J, Ashworth P, Smith GS, Simpson C. 2006. Bartop hollows: A new element in the architecture of sandy braided rivers. *Sedimentary Geology*. 190:241–255
- Bhattacharya PK, Patra HP. 1968. Direct current geoelectric sounding, principles and interpretation. New York: Elsevier Pub. Co; p. 135.
- Binley A, Winship P, Pokar M, West J. 2001. Cross borehole radar and resistivity tomography: a comparison of techniques in unsaturated sandstone. *Symp. applications of geophysics to engineering and environmental problems (SAGEEP)*.
- Bristow CS, Jol HM. 2003. An introduction to ground penetrating radar (GPR) in sediments. *Geological Society*. 211 (1):1–7. doi: 10.1144/GSL.SP.2001.211.01.01
- Burke KC, Freeth SJ, Grant NK. 1976. The structure and sequence of geological events in the basement complex of ibadan area, Western Nigeria, *Prec. Vol. 8, Res.Vol.* p. 6.
- Busby JP, Cuss RJ, Raines MG, Beamish D, 2004: Application of ground penetrating radar to geological investigations. *British Geological Survey Internal Report, IR/04/21*, pp 3.
- Cassidy NJ, Jol H. 2009. Ground penetrating radar data processing, modelling and analysis. In: Jol, HM, editor. *Ground penetrating radar: theory and application*. Elsevier: Amsterdam; p. 141–176
- Comas X, Terry N, Slater L, Warren M, Kolka R, Kristiyono A, Sudiana N, Nurjaman D, Darusman T. 2015. Imaging tropical peatlands in Indonesia using ground-penetrating radar (GPR) and electrical resistivity imaging (ERI): implications for carbon stock estimates and peat soil characterization. *Biogeosciences*. 12 (10):2995–3007. doi:10.5194/bg-12-2995-2015.
- Conyers LB, Goodman D. 1997. *Ground penetrating radar: an introduction for archaeologists: walnut. Creek (CA)*: Alta Mira Press; p. pp. 232.
- Dan-Hassan MA, Olorunfemi MO. 1999. Hydro-geophysical investigation of a basement terrain in the north central part of Kaduna State, Nigeria. *J of Minning Geology*. 35(2):189–206.
- Dara R, Kettridge N, Rivett MO, Krause S, Gomez-Ortiz D. 2019. Identification of floodplain and riverbed sediment heterogeneity in a meandering UK lowland stream by ground penetrating radar. *J Appl Geophys*. 171:103863. doi:10.1016/j.jappgeo.2019.103863.
- Davis JL, Annan AP. 1992. Applications of ground penetrating radar to mining, groundwater, and geotechnical projects: selected case histories; in *Ground penetrating radar*. editor, Pilon J. Geological Survey of Canada, Paper, Vol. 904. 49–55
- Doolittle JA, Collins ME. 1995. Use of soil information to determine application of ground penetrating radar. *J Appl Geophys*. 33(1):101–108. doi:10.1016/0926-9851(95)90033-0.
- Dugan PJ. 1990. Wetland Conservation: A review of Current Issue and Action. *Gland: IUCN*; p. 19–30.



- Ekcs C, Hickin EJ. 2001. Ground penetrating radar facies of the paraglacial Cheekye Fan, southwestern British Columbia, Canada. *Sedimentary Geology*. 143(3--4):199–217. doi:10.1016/S0037-0738(01)00059-8.
- Fagbami A, Ajayi FO. 1990. Valley bottom soils of the sub-humid tropical Southwestern Nigeria on basement complex: characteristics and classification. *Soil Science and Plant Nutrition*. 36(2):179–194. doi:10.1080/00380768.1990.10414983.
- Gourry JC, Vermeersch F, Garcin M, Giot D. 2003. Contribution of geophysics to the study of alluvial deposits: a case study in the Val d'Avaray area of the River Loire, France. *J Appl Geophys*. 54:35–49. doi:10.1016/j.jappgeo.2003.07.002.
- Harry MJ. 2009. Ground penetrating radar: theory and application. Elsevier Science Ltd; p. 544s. eBook ISBN: 9780080951843.
- Heteren SV, Fitzgerald DM, McKinlay PA, Buynevich IV. 1998. Radar facies of paraglacial barrier systems: coastal New England, USA. *Sedimentology*. 45(1):181–200. doi:10.1046/j.1365-3091.1998.00150.x.
- Hong WT, Kang S, Lee SJ, Lee JS. 2018. Analyses of GPR signals for characterization of ground conditions in urban areas. *J Appl Geophys*. 152:65–76. doi:10.1016/j.jappgeo.2018.03.005.
- Ikah NP, Permanasari M, Fadli A, Gunawan H, Lilik H. 2009. Determination of the type of soil using 2d geoelectric method and laboratory analysis for landslide area cililin west java. *Journal of Physics: Conf*. 1127: 1–6. Series.
- Jones HA, Hockey RD. 1964. The geology of part of Southwestern Nigeria: Nigeria Geol. Surv Bull. 31:87.
- Koefoed O. 1979. Geosounding principles, 1. resistivity sounding measurements. In: *Methods in geochemistry and geophysics*. Amsterdam: 14A, Elsevier; p. 272.
- Leclerc RF, Hickin EJ. 1997. The internal structure of scrolled floodplain deposits based on ground-penetrating radar, north thompson river, British Columbia. *Geomorphology*. 21(1):17–38. doi:10.1016/S0169-555X(97)00037-8.
- Lejzerowicz A, Kowalczyk S, Wysocka A. 2014. The usefulness of ground-penetrating radar images for the research of a large sand-bed braided river: case study from the Vistula River (central Poland). *Geologos*. 20:35–47.
- McGinnis LD, Jensen TE. 1971. Permafrost – hydrogeologic regimen in two ice-free valleys, Antarctica, from electrical depth sounding. *Quaternary Research*. 1(3):389–409. doi:10.1016/0033-5894(71)90073-1.
- Mellet JS. 1995. Ground penetrating radar applications in engineering, environmental management, and geology. *J Appl Geophys*. 33(1–3):157–166. doi:10.1016/0926-9851(95)90038-1.
- Minet J, Wahyudi A, Bogaert P, Vanclooster M, Lambot S. 2011. Mapping shallow soil moisture profiles at the field scale using full-waveform inversion of ground penetrating radar data. *Geoderma*. 161(3–4):225–237. doi:10.1016/j.geoderma.2010.12.023.
- Mitchum R, Vail P, Sangree J. 1977. Stratigraphic interpretation of seismic reflection patterns in depositional sequences. In: Payton CE, editor. *Seismic stratigraphy—applications to hydrocarbon exploration*, Vol. 16. AAPG Mem; p. 117–123.
- Mokma DL, Schaetzl RJ, Doolittle JA, Johnson EP. 1990. Ground-penetrating radar study of ortstein continuity in some michigan haplaquods. *Soil Sci Society of America J*. 54(3):936–938. doi:10.2136/sssaj1990.03615995005400030056x.
- Neal A. 2004. Ground-penetrating radar and its use in sedimentology: principles, problems and progress. *Earth-Sci Reviews*. 66(3–4):261–330. doi:10.1016/j.earscirev.2004.01.004.
- Nigeria Geological Survey Agency. 2009. Nigeria Geological Survey Agency (N. G. S. A.). In: *The Geological Map of Nigeria*. Abuja (Nigeria): A publication of Nigeria Geological Survey Agency.
- Nigerian Meteorological Agency (NiMet). 2008. Nigeria climate review bulletin 2007. Nigerian Meteorological Agency NIMET-No. 001
- Nigerian Meteorological Agency (NiMet). 2011. Nigerian meteorological agency, daily weather guide. Nigeria Television Authority. Lagos (Nigeria)
- Oladunjoye MA, Adefehinti A, Ganiyu KAO. 2019. Geophysical appraisal of groundwater potential in the crystalline rock of Kishi area Southwestern Nigeria. *J of African Earth Sci*. 11:1–26.
- Olayinka AI. 1996. Non uniqueness in the interpretation of bedrock resistivity from sounding curves and its hydrological implications. *Water Resources J*. 7(1&2):55–56.
- Olorunfemi MO, Okhue ET. 1991. Electrical resistivity investigation of a typical basement complex area- the obafemi awolowo university campus case study. *J of Mining Geology*. 27(2):66–70.
- Omosuyi GO, Ojo JS, Enikanselu PA. 2003. Geophysical investigation for groundwater around obanla – obakekere in akure area within the basement complex of southwestern Nigeria. *J of Geo and Mining*. 39(2):109–116.
- Orellana E, Mooney HM. 1969. Master curves for schlumberger arrangement. Madrid: 34.
- Palacky GJ, Ritsema IL, De Long SJ. 1981. Electromagnetic prospecting for groundwater in pre-cambrian terrains in the republic of upper volta. *Geophysical Prospecting*. 29(6):932–955. doi:10.1111/j.1365-2478.1981.tb01036.x.
- Poole FG, Page WR, Amaya-Martínez R. 1997. Newly discovered silurian carbonate-shelf rocks in west-central sonora, Mexico: geological society of America abstracts with programs. 29(6):483.
- Reynolds JM. 1987. The role of surface geophysics in the assessment of regional groundwater potential in northern Nigeria in planning and engineering geology. Vol. 4, Geological Society Engineering Group Special Publication. p. 185–190.
- Reynolds JM. 1997. An introduction to applied and environmental geophysics. ChichesterNew York: John Wiley; p. p 796.
- Reynolds JM, Paren JG. 1980. Recrystallization and electrical behavior of glacier ice. *Nature*. 283(5742):63–64. doi:10.1038/283063a0.
- Reynolds JM, Paren JG. 1984. Electrical resistivity of ice from the Antarctic Peninsula. *J of Glaciology*. 30 (106):289–295. doi:10.1017/S0022143000006110.
- Roggeri H. 1995. Tropical Freshwater Wetlands: A Guide to Current Knowledge and Sustainable Management. Dordrecht: Kluwer; p. p 365.
- Samouëlian A, Cousin I, Tabbagh A, Bruand A, Richard G. 2005. Electrical resistivity survey in soil science: a review. *Soil and Tillage Research*. 83(2):173–193. doi:10.1016/j.still.2004.10.004.
- Scott I, Emily P. 2009. Preferential groundwater seepage in karst terrane inferred from geoelectric measurements. *Near Surface Geophysics*. 1–21.
- Silvius MJ, Oneka M, Verhagen A. 2000. Wetlands: lifelines of People at the Edge. *Phy and Chemiof the Earth Part B*. (25):645–652. doi:10.1016/S1464-1909(00)00079-4.

- Stuip MM, Baker CJ, Oostenberg W. 2002. The Socio-economics of wetlands, Wetland International and RIZA. Netherlands: The Netherlands; p. p 35.
- Telford WM, Geldart LP, Sheriff RE. 1990. Applied Geophysics. 3rd Edition ed. Cambridge University Press; p. 770.
- Theimer BD, Nobes DC, Warner BG. 1994. A study of the geoelectrical properties of peatlands and their influence on ground-penetrating radar surveying. *Geophysical Prospecting*. 42:179–209. doi:[10.1111/j.1365-2478.1994.tb00205.x](https://doi.org/10.1111/j.1365-2478.1994.tb00205.x).
- Topp GC, Davis J, Annan AP. 1980. Electromagnetic determination of soil water content: measurements in coaxial transmission lines. *Water Resour Res*. 16(3):574–582. doi:[10.1029/WR016i003p00574](https://doi.org/10.1029/WR016i003p00574).
- Van Dam RL, Schlager W. 2000. Identifying causes of ground-penetrating radar reflections using time-domain reflectometry and sedimentological analyses. *Sedimentology*. 47:435–449. doi:[10.1046/j.1365-3091.2000.00304.x](https://doi.org/10.1046/j.1365-3091.2000.00304.x).
- Wopereis MCS, Defoer T, Idinoba P, Diack S, Dugué MJ. 2009. Participatory learning and action research (PLAR) for integrated rice management (irm) in inland valleys of sub-saharan africa: *technical manual*. In: WARDA training series. Cotonou: Africa Rice Center; p. 128 p.
- Zohdy AAR. 1965. The use of Schlumberger and Equatorial soundings in groundwater investigations near El Paso, Texas. *Geophysics*. 34:713–728. doi:[10.1190/1.1440042](https://doi.org/10.1190/1.1440042).